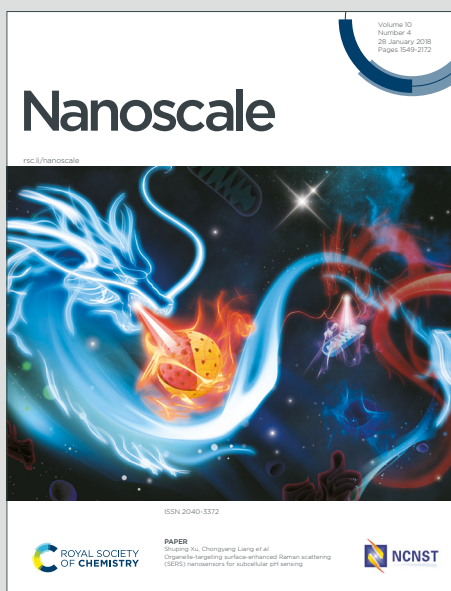


Nanoscale

Accepted Manuscript



This is an Accepted Manuscript, which has been through the Royal Society of Chemistry peer review process and has been accepted for publication.

Accepted Manuscripts are published online shortly after acceptance, before technical editing, formatting and proof reading. Using this free service, authors can make their results available to the community, in citable form, before we publish the edited article. We will replace this Accepted Manuscript with the edited and formatted Advance Article as soon as it is available.

You can find more information about Accepted Manuscripts in the [Information for Authors](#).

Please note that technical editing may introduce minor changes to the text and/or graphics, which may alter content. The journal's standard [Terms & Conditions](#) and the [Ethical guidelines](#) still apply. In no event shall the Royal Society of Chemistry be held responsible for any errors or omissions in this Accepted Manuscript or any consequences arising from the use of any information it contains.

1% defect enriches MoS₂ quantum dot: catalysis and blue luminescence

Jingmin Tang,^a Masanori Sakamoto,^a Haruhisa Ohta,^a and Ken-ichi Saitow^{a,b*}

Received 00th January 20xx,
Accepted 00th January 20xx

DOI: 10.1039/x0xx00000x

Defects in solids are typically recognized as unfavorable, leading to degradation of the structure and properties of the material. However, defects occasionally provide extraordinary benefits as the active sites of catalysts and chemical reactions, and can result in the creation of new electronic states. In particular, a low-dimensional material can become a defect-rich material due to the unique ratio of surface area to volume, giving many dangling bonds. Herein, we report the rapid (20 min) synthesis of MoS₂ quantum dots (QDs) with a diameter of 4 nm at room temperature using nanosecond pulsed laser ablation in a binary solvent. The MoS₂ QDs are crystalline particles composed of 3-5 layers and contain sulfur vacancies at an atomic concentration of 1% acting as a functional defect. The MoS₂ QDs exhibit excellent electrocatalytic performance (Tafel slope = 49 mV/dec) for the hydrogen evolution reaction and high quantum yield blue photoluminescence with a large Stokes shift.

1. Introduction

Two-dimensional transition metal dichalcogenides (2D TMDs) are recognized as materials with excellent physical, electrical, and optical properties. Molybdenum disulphide (MoS₂) is a prototype material in the family of 2D TMDs. The synthesis and exfoliation of low-dimension MoS₂ have been extensively investigated using methods such as mechanical exfoliation,^{1,2} solution-based exfoliation,³ powder sublimation,⁴ thermal decomposition,⁵ solvothermal exfoliation,⁶ chemical vapour deposition (CVD),⁷⁻⁹ and pulsed laser ablation.^{10,11} According to recent studies, MoS₂ nanosheets have excellent electrocatalytic activity for the hydrogen evolution reaction (HER). Defect-rich MoS₂ nanosheets with many sulphur vacancies exhibit particularly high catalytic performance.¹² In contrast, an ideal 2D sheet of a van der Waals material cannot have defects such as dangling bonds, except at the edge of the sheet, whereas their zero-dimensional (0D) and one-dimensional (1D) materials involve a higher density of dangling bonds because of a higher surface/bulk ratio. Therefore, 0D materials, such as quantum dots (QDs), are an ideal material for the HER.

The synthesis of low-dimensional MoS₂ is categorized into top-down and bottom-up methods. Popular top-down methods include exfoliation with sonication³, thermal annealing¹³ and Li intercalation¹⁴. Bottom-up methods such as hydrothermal reaction¹⁵ and CVD⁹ have been extensively used. However, almost all these methods require long times (*ca.* 10-24 h), high temperatures (*ca.* 200°C), and various procedures. These methods can be used to produce 2D sheets; however, it is

difficult to produce QDs of TMDs. Therefore, there have been significantly fewer publications on the synthesis of MoS₂ QDs^{16,17} than on MoS₂ monolayer.

Pulsed laser ablation in liquid (PLAL) is another promising and facile method to obtain stable colloidal nanoparticles (NPs).¹⁸ PLAL is a one-step, one-pot, short (*ca.* 3 min to 1 h) room-temperature process used to synthesize various NPs and QDs.¹⁸⁻²¹ For instance, an electrocatalysis of NPs has been improved by hetero junction,^{21a} and the scalability of NP synthesis has also been demonstrated with synthesis rates as high as 4 g h⁻¹.^{21b,c} PLAL has been previously employed for the synthesis of 2D TMDs, fullerene-like MoS₂ NPs,¹⁰ 2D and 3D nanostructure,¹¹ thin films,²² and QDs have been reported using PLAL.²³⁻²⁵ Although there are two papers on the ultra-small QDs (*ca.* 5 nm) synthesized by PLAL (fs-PLAL),^{24,25} those properties, optical and catalyst, have not been fully understood yet. In addition, the functionality of defects has not been quantified for MoS₂ QDs prepared by all the synthesis methods so far. Under these situations, the synthesis of ultra-small QDs of TMDs is highly desirable to realize a material with a high edge-to-volume ratio that is expected to provide higher catalytic performance for the HER. Furthermore, one-pot, short-time, and room-temperature processes are a promising method to prepare MoS₂ ODs. Herein, we show a simple and facile method to synthesize ultra-small MoS₂ QDs using PLAL in a binary solvent, i.e. ns-PLAL. The average size of the resultant MoS₂ QDs was 4.2 nm and they had good electrocatalytic activity for the HER due to an abundance of sulphur vacancies, whose density was directly quantified by ESR measurements. In addition, blue photoluminescence (PL) of the MoS₂ QDs was observed and the quantum yield was 10⁵ times higher than that of bulk MoS₂. The structures and properties of MoS₂ QDs were evaluated using 9 experimental methods.

2. Experimental section

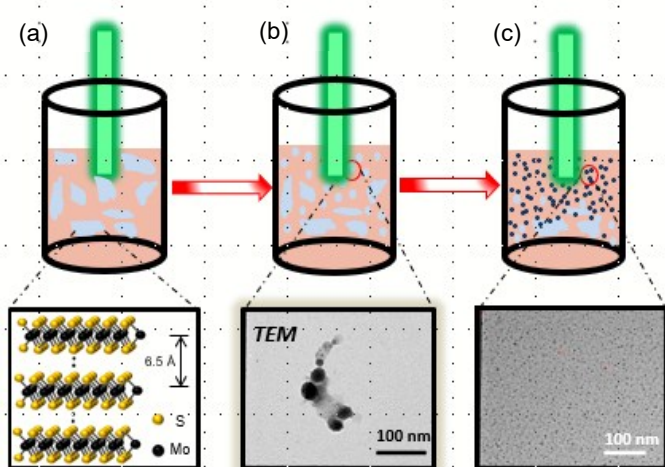
^aDepartment of chemistry, Graduate school of science, Hiroshima University, 1-3-1 Kagamiyama, Higashi-Hiroshima 739-8526, Japan, saitow@hiroshima-u.ac.jp.

^bDepartment of materials science, Natural Science Centre for Basic Research and Development, 1-3-1 Kagamiyama, Higashi-Hiroshima 739-8526, Japan

Electronic Supplementary Information (ESI) available: [Optical configuration of PLAL synthesis, XRD, ESR, and EDX data, and band gap energy vs. size.]. See DOI: 10.1039/x0xx00000x

2.1 Synthesis of MoS₂ QDs

MoS₂ powder with a size of 2 μm was used as purchased (>99%, Sigma Aldrich), and 10 mg was dissolved in a binary solvent of ethanol (9 ml) and distilled water (11 ml). Pulsed laser ablation in liquid (PLAL) was conducted for 20 min using the second harmonic (532 nm, 10 Hz, 7 ns pulse width) of a Nd:YAG laser (Quanta-Ray INDI-series, Spectra Physics) with a fluence of 0.16 J cm⁻². As illustrated in Fig. S1, the laser was directed downward onto the solution and focused on the middle portion. During PLAL, the solution was stirred with a magnetic stirrer at 300 rpm. The solution after PLAL was then centrifuged at 7500 rpm for 0.5 h. The solution taken from the top two thirds was used as a sample and was pure light blue in colour.



Scheme 1 Schematic diagrams of the 3-step PLAL process. a) MoS₂ powders are dispersed in a binary solvent of ethanol and water. b) Solution irradiated with laser pulses for 3–5 min. MoS₂ particles with sizes of 20–50 nm are synthesized. c) MoS₂ QDs with sizes of 2–9 nm are obtained after irradiation for 20 min.

1.2. Characterizations of MoS₂ QDs.

Transmission electron microscopy (TEM) (JEM-2010, JEOL) was performed at an accelerating voltage of 200 kV. TEM samples were prepared by dropping the MoS₂ solution onto a TEM grid in air, and the grid was successively dried in a vacuum oven for 30 min.

Electrochemical measurements were conducted using an electrochemical analyser (ALS600EB, BAS) with a 0.5 M H₂SO₄ solution and Pt, Nafion Ag/AgCl (3 M NaCl), and Pt as the working, reference, and counter electrodes. The scanning range was –0.6 to 0.4 V and the scan rate was 100 mV s⁻¹ for all measurements. The MoS₂ QDs film samples were prepared in the following manner. First, the solvent of the MoS₂ QDs solution was evaporated on a hot plate at 200 °C to obtain the powder. Second, the powder of either MoS₂ QDs or MoS₂ bulk was dissolved in a binary solvent of deionized water and ethanol (4:1 by volume), which included 80 μL Nafion (5 wt%). Then, the solution was sonicated for 30 min. Third, the MoS₂ solution with a volume of 5 μL such as slurry was dropped on the Au electrode,²⁶ followed by drying in a vacuum oven at 30 °C.

Electron spin resonance (ESR) spectra were measured at X-band using powder samples of bulk MoS₂ and MoS₂ quantum

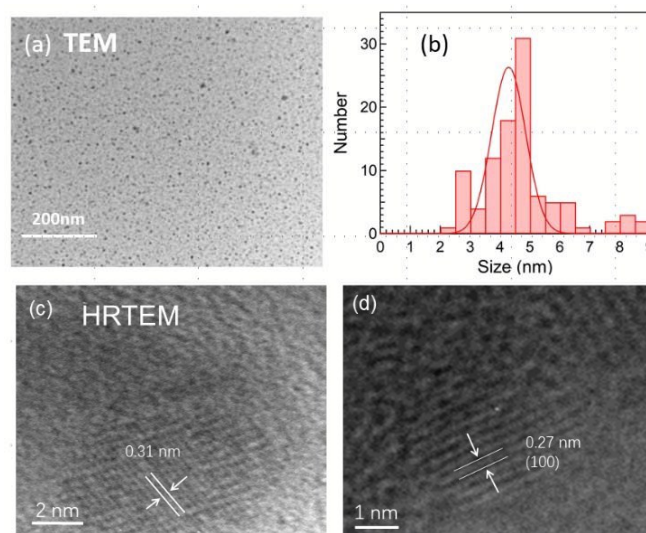


Fig. 1 a) TEM image after PLAL process. b) Size distribution of MoS₂ particles, which is dispersed in the range of 2–9 nm with the average size of 4.2 nm. c, d) HRTEM images of the MoS₂ QDs.

dot (QD) with a commercial instrument (ELEXSYS E500, Bruker). Spin density of MoS₂, density of sulphur vacancy, was estimated from the ratio of integrated spectral area of MoS₂ divided by that of a standard, copper sulphate pentahydrate (CuSO₄•5H₂O), under the condition of the same molar amount. The measurements of the standard were conducted using polycrystalline of CuSO₄•5H₂O, and their area of integrated profiles gave the same values in every measurement (ESI).

The photoluminescence (PL) and PL excitation (PLE) spectra, PL quantum yield (QY), and UV-vis absorption spectra were, respectively, recorded using a fluorometer (FluoroMax-4, Horiba), a spectrometer with an integrating sphere (Quantaury-QY, Hamamatsu), and a spectrometer (V600, JASCO) using MoS₂ QDs dissolved in the binary solvent. Raman spectra of the MoS₂ QDs were measured using a Raman spectrometer (HR800, Horiba Jobin Yvon) at an excitation wavelength of 514.5 nm. The Raman sample was prepared by dropping the MoS₂ solution onto a silicon-wafer substrate, followed by drying for 20 minutes in air.

Regarding the other method, we measured the thickness of MoS₂ QDs using an atomic force microscope (AFM) (SHIMADZU SPM-9700). X-ray diffraction (XRD) patterns were investigated using a commercial diffractometer (Rigaku B/Max-RB) with Ni-filtered Cu Kα radiation. For XRD measurements, we prepared powders of bulk MoS₂ or MoS₂ QDs, which were set onto a silicon sample holder of low intensity background (ESI).

Results and discussion

Schematic diagrams of the PLAL procedure are displayed in Scheme 1. Bulk MoS₂ powders dispersed in the binary solvent is irradiated by the pulsed laser (Scheme 1a). MoS₂ NPs with sizes of 20–50 nm are obtained after a few minutes (Scheme 1b), and a representative TEM image is shown in scheme 1c. Ultra-small MoS₂ QDs are synthesized after laser irradiation for 20 minutes.

Magnified TEM images of synthesized MoS₂ QDs are shown in in Figure 1. The size distribution of MoS₂ QDs ranges in 2–9

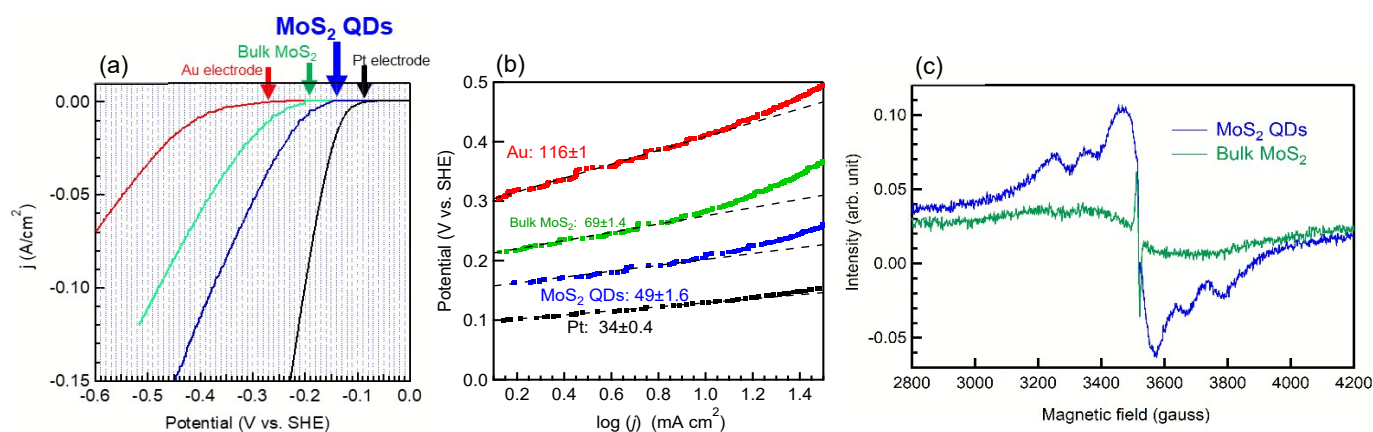


Fig. 2 Characterisation of the HER. a) Polarization curves of Au and Pt electrodes, bulk MoS₂, and MoS₂ QDs deposited on Au electrodes, which were measured in 0.5 M H₂SO₄ at a scan rate of 2 mV/s. b) Tafel plots and Tafel slopes. c) ESR spectra of MoS₂ QDs and bulk MoS₂.

nm (Figure 1b). The average size is 4.2 nm, which is close to the reported Bohr radius for MoS₂ (1–3 nm).^{27,28} According to the definition of QD, i.e., particle radius ≈ Bohr radius of an exciton, the current QD can be confirmed as an actual QD. In addition, the thickness of the MoS₂ QDs was carefully measured with AFM to be 3.6 nm, which corresponds to 3–5 layers (Figure S2). High-resolution TEM (HRTEM) images of the MoS₂ QDs are displayed in Figure 1c–d. Lattice fringes of 0.27 and 0.31 nm spaces are observed, which correspond to the distance between the (100) planes of MoS₂ (0.27 nm).²⁹ Thus, the PLAL method employed in the current study successfully synthesized crystalline MoS₂ QDs. The result of XRD also indicates crystalline MoS₂ QDs (Figure S3). Here, let us note the previous studies on MoS₂ nanomaterials synthesized by PLAL. MoS₂ NPs with 20 nm QDs¹¹ and fullerene-like MoS₂ NPs¹⁰ were obtained from PLAL using methanol and water as solvents, respectively; however, smaller sized TMDs have not been synthesized by ns-PLAL. By

changing the solvent for PLAL in the present study, the particle size was reduced from 20 nm to 4 nm. MoS₂ QDs with an average size of 4 nm by PLAL in a binary solvent composed of water and ethanol were thus obtained. The ultra-small QDs were generated in a binary solvent due to the following: i) a principle reason is the use of a binary solvent, which acts as a good solvent for MoS₂. This is because excellent solubility is established in the 45 vol% ethanol/water mixture,³⁰ which is responsible for the Hansen solubility parameters. ii) A shockwave generated by the initial process of PLAL effectively exfoliates MoS₂ powders with the original size (2 μm) in the good solvent. Water and/or ethanol molecules interact with the edge of the delamination of MoS₂, which triggers exfoliation and fragmentation (*ca.* 50 nm). iii) Subsequent laser shots in the binary solvent continue the process described in ii) which results in sizes smaller than 5 nm, as shown in Figure 1 and S2.

Table 1. Comparison of structures, Tafel slope of HER, synthesis conditions of low-dimensional MoS₂. The listed data^{a)} focus on the top 10 papers as the highest citation, which measure Tafel slope of the MoS₂ of 2H-phase as semiconductor.^{b)}

Structure	Tafel slope (mV/dec)	Method	Temperature (°C)	Time	Note	Ref
^{c)} Nanoparticle	94	Solvothermal	200	> 10 h	Citation # = 2753 (Nov. 7 th , 2019)	35a
Amorphous	40	Electro-polymerization	---	---	This sample is not a low dimensional material but a thin film.	35b
^{d)} Nanoparticle	85	Hydrothermal	200	> 36 h	Particle size = 3–5 nm.	35c
^{e)} Nanoparticle	100	Urea-glass route	750	4 h	Particle size = 5–10 nm	35d
Nanoplate	53	Solvothermal	210, 800	> 44 h	Size = 200–300 nm	35e
Nanoparticle	69	Sonication, centrifugation	R.T.	5 h	Particle size = 1–2 nm	35f
^{f)} Monolayer	50	CVD	750	45 min.	Triangular size = 5–30 μm	35g
Nanoflake	61	CVD	530–750	90 min.	Triangular size = 0.2–50 μm	35h
Nanosheet	68	Ball milling	350–750	> 24 h	Milled samples were annealed at high temperature.	35i
Thin film	65–160	CVD	700–900	---	Sulfur vacancies were analyzed by XPS and discussed with the value of Tafel slope.	35j
Quantum dot	49	Pulsed laser ablation	R.T.	20 min.	Present study, particle size = 3–5 nm	---

^{a)} The data are given by the top 10 papers as the highest citations of MoS₂ HER, based on the analysis of the SciFinder scholar using the keyword of MoS₂ and Tafel. The data in the table are listed by the order of citation number.

^{b)} Metallic MoS₂, 1T-phase, and the binary system between MoS₂ and the other material show smaller Tafel slope (*ca.* 45 mV/dec) in several papers, i.e. refs. 35a and 35c.

^{c)} The system of MoS₂/RGO (reduced graphene oxide) shows smaller Tafel slope.

^{d)} The system of MoS₂/mesoporous-graphene-form shows smaller Tafel slope.

^{e)} This MoS₂ is attached on carbon nanotubes.

^{f)} The metallic phase, 1-T MoS₂, is also studied.

In fact, larger-sized particles are produced by PLAL with either pure water or other neat organic solvents in the present study.

To evaluate the catalytic properties of ultra-small MoS₂ QDs, electrochemical measurements for the HER were conducted, and the results for MoS₂ were compared with those for bulk MoS₂ and noble metals. Current density vs. the electric potential applied to these materials is shown in Figure 2a. The HER starts at the position where the voltage drops, and the HER over MoS₂ QDs occurs at a lower voltage than those of Au and bulk MoS₂. This indicates that MoS₂ QDs act as better electrocatalysts. To quantify the catalytic properties, Tafel plots were analysed, as shown in Figure 2b. The MoS₂ QDs have a very small Tafel slope of 49±1.6 mV/dec. A smaller Tafel slope indicates better catalysis of the HER; therefore, the MoS₂ QDs prepared in the present study act as a very good catalyst. Very good electrocatalytic performance of MoS₂ has been reported for low-dimensional MoS₂, i.e., Tafel slopes of 50 mV/dec for defect-rich nanosheets,^{12a} 87 mV/dec for defect-free

nanosheets,^{12a} and 69 mV/dec³¹ and 98 mV/dec³² for QDs. Note that the Tafel slope for the MoS₂ QDs in the present study (49±1.6 mV/dec) is almost same as that for defect-rich nanosheets (50mV/dec).¹² The excellent electrocatalysis of defect-rich MoS₂ nanosheets is attributed to sulphur (S) vacancies at active sites.^{12,33,34a,c} Furthermore, we compared the current study with the top 10 papers of the highest citation (table 1) of MoS₂ HER.³⁵ Therefore, the current study shows very good Tafel slope and the shortest synthesis time of MoS₂ nanomaterials.

To evaluate the defects in the present system, we conducted ESR spectroscopy measurements, indicating a direct observation of defect as a spin active species. The results are shown in Figure 2c. The ESR spectrum of MoS₂ QDs is in very good agreement with that of MoS₂ with S vacancies,^{12,34} and also has the same g-value of 2.00.³⁴ The MoS₂ QDs in the current study have S vacancies, which also give excellent catalytic properties and are consistent with the study on defect-rich

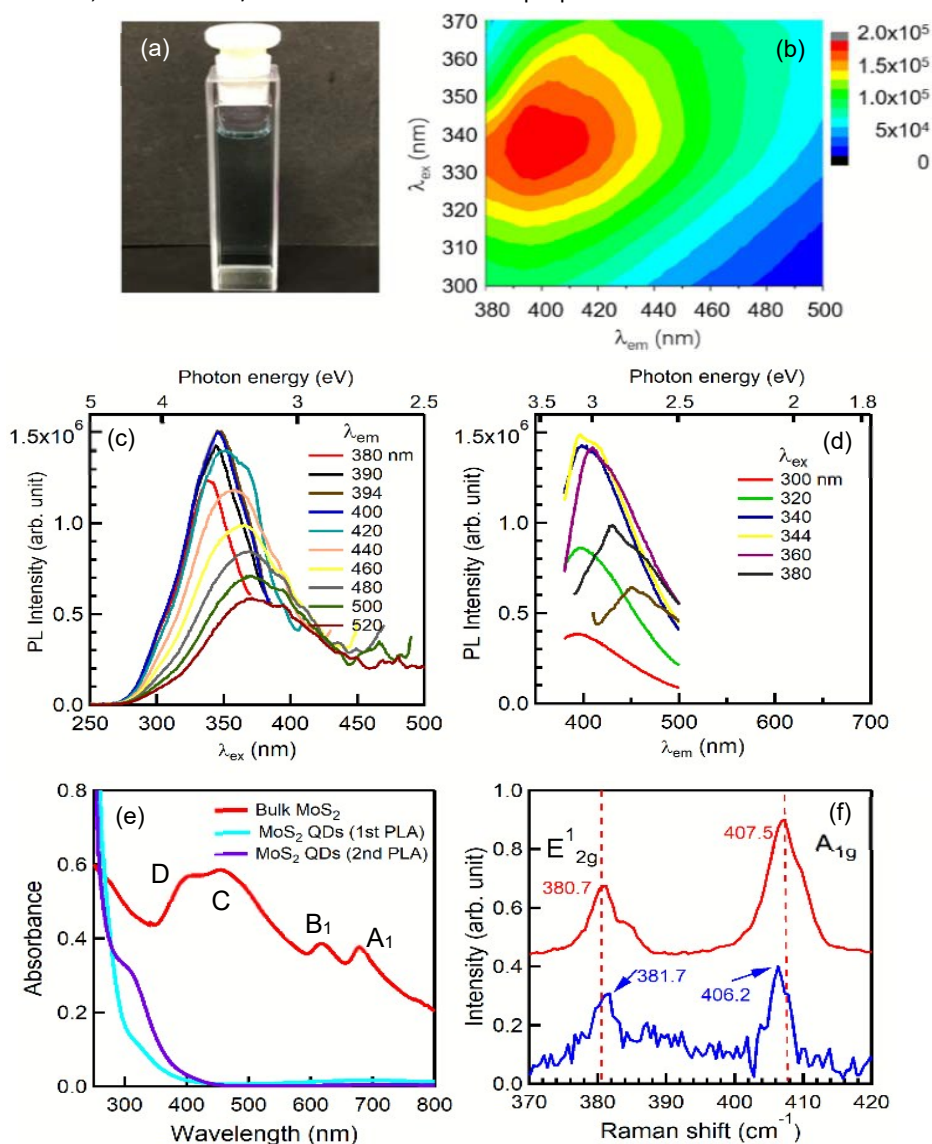


Fig. 3 a) Photograph is MoS₂ QDs in solution with a transparent blue colour. b) 3D map of PL and PLE. c) PLE and d) PL spectra of MoS₂ QDs. e) UV-vis absorption spectra of bulk MoS₂ and MoS₂ QDs. f) Raman spectra of bulk (red) and MoS₂ QDs (blue). The arrows denote peak positions of the bands.

MoS₂ nanosheets.¹² Furthermore, this is the first time that the atomic concentration of S vacancy is quantified by measuring spin density and its value is 1% (Figure S4). Therefore, it was found that 1% of a point defect in MoS₂ act as an excellent functional defect for HER.

Next, the electronic structure of MoS₂ was evaluated through PL, PLE, and UV-vis absorption spectroscopy measurements. A photograph, PL-PLE map, PL, and PLE spectra of a solution of MoS₂ QDs are shown, in Fig. 3 respectively. The PL spectra range from 400 to 500 nm for the luminescence in the blue region. The peak position shifts to longer wavelengths with the excitation wavelength, which indicates that, the MoS₂ QDs with different band gap E_g and different size QDs exhibit different PL wavelengths when excited (*vide infra*). To evaluate the spectral shapes, PL (Figure 3c) and PLE (Figure 3d) spectra are displayed as functions of the wavelength and photon energy. Thus, a mirror image between PL and PLE spectra is evident. Note that the peak positions of PL and PLE are located at around 400 and 350 nm, respectively, and there is a large Stokes shift, i.e., =50 nm, which corresponds to 0.44 eV. Such a large Stokes shift has been observed in graphene QDs, and this large shift is useful for application as a down converter material for solar cells.³⁶ Another distinct result is that the PL quantum yield (QY) of MoS₂ QDs is 3.8%, whereas those of bulk MoS₂ and monolayer MoS₂ have been reported to be almost 0%¹ and 0.4%¹, respectively. Thus, the QY of the MoS₂ QDs here is almost 10 times higher than that of the MoS₂ monolayer. The reason for the high QY of monolayer MoS₂ has been recognized as a high rate of electron-hole recombination in a confined system, such as a 2D monolayer.³⁷ Taking the current size into account (4.2 nm \approx Bohr radius, 1-3 nm),^{27, 28} a higher recombination rate is expected to occur in a further confined system, such as a 0D material.

UV-vis absorption spectra of bulk MoS₂ and the MoS₂ QDs are shown in Figure 3e. Four bands are observed in bulk MoS₂ at around 678, 618, 454, and 410 nm, the two former bands are named as A1 and B1 bands, which are attributed to the direct transitions from the top of the valence band to two excitonic states, spin-orbit splitting, at the Brillouin zone K point.^{38,39} The two latter bands are named C and D bands, which are attributed to a direct transition from deeper levels in the valence band to two excitonic states, spin-orbit splitting at the Brillouin zone M point.³⁸ In the UV-vis absorption spectrum of MoS₂ QDs, there are two shoulders at around 340 and 370 nm, the positions of which are in agreement with those of the PLE spectrum for MoS₂ QDs shown in Figure 3d. Furthermore, these positions at 3.65 eV and 3.35 eV are in good agreement with the B₁ and A₁ bands of MoS₂ nanoclusters with a size of 3-4 nm, according to reported experimental data of size vs. UV-vis absorption peak energy,^{38a} as shown in Fig. S6b. Based on these situations, the two bands (340 nm, 3.65 eV; 370 nm, 3.35 eV) in the PLE and UV-vis absorption spectra are attributed to the transitions of two excitonic states at the K point. Therefore, the PL spectra in Figures 3c, result in luminescence via the transition of A₁ and B₁ bands, shifting into the blue wavelength region, to give a high QY (3.8%). Finally, the dependence of E_g on the size of the MoS₂ QDs was evaluated using the data of the size of MoS₂

nanoclusters vs. UV-vis absorption band (*vide supra*).^{38a} Size distribution, the full width at half maximum (FWHM) in Figure 1b, was 3.7-4.9 nm, which gave $E_g = 3-4$ eV, i.e. $E_g=2.8-3.2$ eV (A₁) and 3.4-3.7 eV (B₁), according to Fig. S6b. Note that this energy range is almost equal to the FWHM of the PLE spectra, i.e., 3.4 eV (370 nm)–3.9 eV (320 nm), as shown in Figure 3d.

As a final topic, let us note the Raman spectrum of bulk MoS₂ and the MoS₂ QDs. The lower and higher frequency bands have been attributed to the in-plane E_{2g} and out-of-plane A_{1g} modes, respectively, and the increment between the bands is an indicator of layer thickness.^{41,42} A narrower increment is shown in the MoS₂ QDs (Figure 3f), i.e., bulk MoS₂ is 26.8 cm⁻¹, whereas that of MoS₂ QDs is 24.5 cm⁻¹, which corresponds to 3-5 layers. This layer size is consistent with the height measured by AFM and the size of MoS₂ QDs by TEM.

Conclusions

In summary, we demonstrated a fast and facile method to obtain uniform-sized MoS₂ QDs using PLAL in the binary solvent. The aqueous solution of 45% ethanol played a critical role in the synthesis of ultra-small MoS₂ QDs with an average size of 4 nm. These QDs showed excellent electrocatalytic performance for the HER with a very small Tafel slope (49mV dec⁻¹), which was attributed to many sulphur vacancies as much as 1%. The excitons confined in the 4 nm MoS₂ QDs caused blue PL and the efficient recombination among electrons and holes. The PL QY for the MoS₂ QDs was 3.8%, which was almost 10 times higher than that for MoS₂ monolayer. The present study demonstrated very good electrocatalyst for HER, the shortest synthesis time of QDs, and room-temperature process in comparison with the top 10 papers as the highest citations as the HER of MoS₂.

Conflicts of interest

There are no conflicts to declare.

Acknowledgements

K.S. acknowledges financial support from the Funding Program for the Next Generation World-Leading Researchers (GR073) of the Japan Society for the Promotion of Science (JSPS), a Grant-in-Aid for Scientific Research (A) (15H02001) and (B) (19H02556) from JSPS, the PRESTO Structure Control and Function program of the Japan Science and Technology Agency (JST), and JKA through its promotion funds from AUTORACE. We acknowledge Dr. Maeda for measuring TEM images and Mrs. Kawata for measuring ESR spectra at N-BARD Hiroshima University.

Notes and references

- 1 K. F. Mak, C. Lee, J. Hone, J. Shan and T. F. Heinz, *Phys. Rev. Lett.*, 2010, **105**, 136805.
- 2 A. Splendiani, L. Sun, Y. Zhang, T. Li, J. Kim, C. Y. Chim, G. Galli and F. Wang, *Nano Lett.*, 2010, **10**, 1271.

- 3 a) J. N. Coleman, and V. Nicolosi et al, *Science.*, 2011, **331**, 568. b) M. Sakamoto, K. Saitow, *Nanoscale*, 2018, **10**, 22215.
- 4 W.K. Hsu, B.H. Chang, Y.Q. Zhu, W.Q. Han, H. Terrones, M. Terrones, N. Grobert, A.K. Cheetham, H.W. Kroto, D.R. Walton, *J. Am. Chem. Soc.*, 2000, **122**, 10155.
- 5 S. Balendhran, J. Z. Ou, M. Bhaskaran, S. Sriram, S. Ippolito, Z. Vasic, E. Kats, S. Bhargava, S. Zhuiykov and K. Kalantar-zadeh, *Nanoscale*, 2012, **4**, 461.
- 6 Z. Liu, Y. B. Wang, Z. Y. Wang, Y. G. Yao, J. Q. Dai, S. Das and L. B. Hu, *Chem. Commun.*, 2016, **52**, 5757.
- 7 Y. Zhan, Z. Liu, S. Najmaei, P.M. Ajayan, J. Lou, *Small.*, 2012, **8**, 966.
- 8 Y. C. Lin, W. J. Zhang, J. K. Huang, K. K. Liu, Y. H. Lee, C. T. Liang, C. W. Chu and L. J. Li, *Nanoscale*, 2012, **4**, 6637.
- 9 J. Jeon, S. Jang, S. Jeon, G. Yoo, Y. Jang, J.-H. Park and S. Lee, *Nanoscale*, 2015, **7**, 1688.
- 10 H.H. Wu, R. Yang, B.M. Song, Q.S. Han, J.Y. Li, Y. Zhang, Y. Fang, R. Tenne and C. Wang, *ACS Nano.*, 2011, **5**, 1276.
- 11 T. Oztas, H. S. Sen, E. Durgun, B. Ortac, *J. Phys. Chem. C.*, 2014, **118**, 30120.
- 12 a) J. Xie, H. Zhang, S. Li, R. Wang, X. Sun, M. Zhou, J. Zhou, X.W. Lou, Y. Xie, *Adv Mater.*, 2013, **25** 5807. b) G. Ye, Y. Gong, J. Lin, B. Li, Y. He, S. T. Pantelides, W. Zhou, R. Vajtai, P. M. Ajayan, *Nano Lett.* 2016, **16**, 1097.
- 13 X. Lu, M. I. Utama, J. Zhang, Y. Zhao and Q. Xiong, *Nanoscale*, 2013, **5**, 8904.
- 14 Y. W. Lihui, H. Yu, X. R. Yang, J. J. Zhou, Q. Zhang, Y. Q. Zhang, Z. M. Luo, S. Su and L. H. Wang, *Chem. Commun.*, 2016, **52**, 529.
- 15 D.Z. Wang, Z. Pan, Z. Z. Wu, Z.P. Wang, Z.H. Liu, *J. Power Sources.*, 2014, **264**, 229.
- 16 a) Deepesh, G., Dijo, D. & Shaijumon, M. M. *Acs Nano.* 8, 5297 (2014), b) Xu, S., Li, D. & Wu, P, *Adv. Funct. Mater.* 2015, **25**, 1127. c) D. Gopalakrishnan, D. Damien, B. Li, H. Gullappalli, V. K. Pillai, P. M. Ajayan and M. M. Shaijumon, *Chem. Commun.*, 2015, **51**, 6293.
- 17 Publications were surveyed by SciFinder scholar. Specifically, the number of publications of studies on “MoS₂ quantum dot” and “MoS₂ monolayer” were 33 and 544, both of which were analysed by selecting document type (paper, letter, and review) and language (English).
- 18 a) D. Zhang, B. Gökce, S. Barcikowski, *Chem. Rev.*, 2017, **117**, 3990. b) B. Gökce, V. Amendola, S. Barcikowski, *ChemPhysChem*, 2017, **18**, 983. c) D. Zhang, J. Liu, P. Li, Z. Tian, C. Liang, *ChemNanoMat*, 2017, **3**, 512. d) M. R. Kalus, R. Lanyumba, N. Lorenzo-Parodi, M. A. Jochmann, K. Kerpen, U. Hagemann, T. C. Schmidt, S. Barcikowski, B. Gökce, *Phys. Chem. Chem. Phys.*, 2019, **21**, 18636.
- 19 a) D. Kajiya, K. Saitow., *RSC Adv.*, 2018, **8**, 41299. b) Y. Xin, T. Kitasako, M. Maeda, and K. Saitow, *Chem. Phys. Lett.*, 2017, **674**, 90. c) Y. Xin, K. Nishio and K. Saitow, *Appl. Phys. Lett.*, 2015, **106**, 201102. d) T. Kitasako and K. Saitow, *Appl. Phys. Lett.*, 2013, **103**, 151912.
- 20 a) K. Saitow, Y. Okamoto, H. Suemori, *ACS Omega*, 2019, **4**, 14307. b) S. Wei, T. Yamamura, D. Kajiya, K. Saitow, *J. Phys. Chem. C* 2012, **116**, 3928; c) K. Saitow, Y. Okamoto, Y. F. Yano, *J. Phys. Chem. C.*, 2012 **116**, 17252, d) K. Saitow, T. Yamamura, *J. Phys. Chem. C.*, 2009, **113**, 8465, e) K. Saitow, T. Yamamura, T. Minami, *J. Phys. Chem. C*, 2008, **112**, 18340; f) K. Saitow, *J. Phys. Chem. B.*, 2005, **109**, 3731.
- 21 a) J. Lv, S. Wu, Z. Tian, Y. Ye, J. Liu & C. Liang, *J. Mater. Chem. A*, 2019, **7**, 12627-12634. b) C. L. Sajti, R. Sattari, B. N. Chichkov, S. Barcikowski, *Appl. Phys. A*, 2010, **100**, 203, c) Y. Ishikawa, N. Koshizaki, *Sci. Rep.*, 2018, **8**, 14208.
- 22 S. Alkis, T. Öztas, L. E. Aygün, F. Bozkurt, A. K. Okyay, & B. Ortac, *J. Optics express*, 2012, **20**, 21815.
- 23 H. G. Baldoví, M. Latorre-Sánchez, I. Esteve-Adell, A. Khan, A. M. Asiri, S. A. Kosa, H. Garcia, *J. Nanoparticle Res.* 2016, **18**, 240.
- 24 G. Ou, P. Fan, X. Ke, Y. Xu, K. Huang, H. Wei, W. Yu, H. Zhang, M. Zhong, H. Wu, Y. Li, *Nano Res.*, 2018, **11**, 751.
- 25 V. Nguyen, Q. Dong, L. Yan, N. Zhao, P. H. Le, *J. Lumines.* 2019, **214**, 116554.
- 26 Z.Z. Wu, B.Z. Fang, D.Z. Wang, D.P. Wikinson et al, *ACS Catal.* 2013, **3**, 2101.
- 27 R. Doolen, R. Laitinen, F. Parsapour, and D. F. Kelley, *J. Phys. Chem. B.*, 1998, **102**, 3906.
- 28 (a) R. Li, X. Dong, Z. Li, Z. Wang, *Solid State Commun.*, 2018, **275**, 53. (b) M.L. Trolle, T.G. Pedersen, V. Vénard, *Sci. Rep.* 2017, **7**, 39844.
- 29 Y. H. Lee, X. Q. Zhang, W. Zhang, M. T. Chang, C. T. Lin, K. D. Chang, Y. C. Yu, J. T.-W. Wang, C. S. Chang, L. J. Li and T. W. Lin, *Adv. Mater.*, 2012, **24**, 2320.
- 30 K. G. Zhou, N. N. Mao, H. X. Wang, Y. Peng, & H. L. Zhang, *Angew. Chem. Int. Ed*, 2011, **50**, 10839.
- 31 S. Das, R. Ghosh, P. Routh, A. Shit, S. Mondal, A. Panja and A. K. Nandi, *ACS Appl. Nano Mater.*, 2018, **1**, 2306
- 32 L. Najafi, S. Bellani, B. Martín-García, R. Oropesa-Nuñez, A. E. Del Rio Castillo, M. Prato, I. Moreels and F. Bonaccorso, *Chem. Mater.*, 2017, **29**, 5782.
- 33 G. Li, D. Zhang, Q. Qiao, Y. Yu, D. Peterson, A. Zafar, R. Kumar, S. Curtarolo, F. Hunte, S. Shannon, Y. Zhu, W. Yang and L. Cao, *J. Am. Chem. Soc.*, 2016, **138**, 16632.
- 34 a) B. Deroide, Y. Bensimon, P. Belougne, J. V. Zanchetta, *J. Phys. Chem. Solids*, 1991, **52**, 853. b) Y. Yin, J. Han, Y. Zhang, X. Zhang, P. Xu, Q. Yuan, L. Samad, X. Wang, Y. Wang, Z. Zhang, P. Zhang, X. Cao, B. Song, and S. Jin, *J. Am. Chem. Soc.* 2016, **138**, 7965. c) L. Cai, J.F. He, Q.H. Liu, T. Yao, L. Chen, W. S. Yan, F.C. Hu, Y. Jiang, Y.D. Zhao, T.D. Hu, Z.H. Sun, S.Q. Wei, *J. Am. Chem. Soc.*, 2015 **137**, 2622.
- 35 a) Y. Li, H. Wang, L. Xie, Y. Liang, G. Hong, H. Dai, *J. Am. Chem. Soc.* 2011, **133**, 7296. b) D. Merki, S. Fierro, H. Vruble, X. Hu, *Chem. Sci.*, 2011, **2**, 1262. c) L. Liao, J. Zhu, X. Bian, L. Zhu, M. D. Scanlon, H. H. Girault, B. Liu, *Adv. Funct. Mater.* 2013, **23**, 5326. d) D. H. Youn, S. Han, J. Y. Kim, J. Y. Kim, H. Park, S. H. Choi, J. S. Lee, *ACS nano*, 2014, **8**, 5164. e) Y. Yan, B.Y. Xia, X. Ge, Z. Liu, J. Wang, X. Wang, *ACS Appl. Mater. Interfaces* 2013, **5**, 12794. f) T. Wang, L. Liu, Z. Zhu, P. Papakonstantinou, J. Hu, H. Liu, M. Li, *Energy Environ. Sci.*, 2013, **6**, 625. g) D. Voiry, R. Fullon, J. Yang, C. d. C. e Silva, R. Kappera, I. Bozkurt, D. Kaplan, M. J. Lagos, P. E. Batson, G. Gupta, A. D. Mohite, L. Dong, D. Er, V. B. Shenoy, T. Asefa, M. Chhowalla, *Nat. Mater.*, 2016, **15**, 1003. h) J. Shi, D. Ma, G. Han, Y. Zhang, Q. Ji, T. Gao, J. Sun, X. Song, C. Li, Y. Zhang, X. Lang, Y. Zhang, Z. Liu, *ACS nano*, 2014, **8**, 10196. j) Z. Wu, B. Fang, Z. Wang, C. Wang, Z. Liu, F. Liu, W. Wang, A. Alfantazi, D. Wang, D. P. Wilkinson, *ACS Catal.* 2013, **3**, 2101. i) G. Li, D. Zhang, Q. Qiao, Y. Yu, D. Peterson, A. Zafar, R. Kumar, S. Curtarolo, F. Hunte, S. Shannon, Y. Zhu, W. Yang, L. Cao, *J. Am. Chem. Soc.* 2016, **138**, 16632.
- 36 F. Khan, J.H. Kim. *ACS Photo.*, 2018, **5**, 4637.
- 37 M. Amani, D. Lien, D. Kiriya, J. Xiao, A. Azcatl, J. Noh, S.R. Madhvapathy, R. Addou, S. Kc, M. Dubey, K. Cho, R.M. Wallace, S. Lee, J. He, J.W.A. Iii, X. Zhang, E. Yablonovitch, A. Javey. *Science* 2015, **350**, 1065.
- 38 a) J.P. Wilcoxon, P.P. Newcomer, G. A. Samara. *J. Appl. Phys.*, 1997, **81**, 7934. b) R. F. Frindt, A. D. Yoffe, *Proc. R. Soc. London, Ser. A* 1963, **273**, 69. c) A. Splendiani, L. Sun, Y. Zhang, T. Li, J. Kim, C. Chim, G. Galli, F. Wang, *Nano Lett.* 2010, **10**, 1271. d) R. F. Frindt, *Phys. Rev.* 1965, **140**, A536. e) G. Eda, H. Yamaguchi, D. Voiry, T. Fujita, M. Chen, M. Chhowalla, *Nano Lett.* 2011, **11**, 5111. f) R. Ahmad, R. Srivastava, S. Yadav, D. Singh, G. Gupta, S. Chand, S. Sapra, *J. Phys. Chem. Lett.* 2017, **8**, 1729.
- 39 The optical transitions of A1 and B1 are considered as direct transitions for monolayer, whereas those of a bulk MoS₂ are attributed as indirect transitions, described in refs. 38c and 40.

- 40 a) K. F. Mak, C. Lee, J. Hone, J. Shan, T. F. Heinz, *Phys. Rev. Lett.*, 2010, **105**, 136805. b) A. Molina-Sánchez, D. Sangalli, K. Hummer, A. Marini, L. Wirtz, *Phys. Rev. B* 2013, **88**, 045412.
- 41 Radisavljevic, A. Radenovic, C. Lee, H. Yan, L. Brus, T. F. Heinz, J. Mone, S. Ryu, *ACS Nano*, 2010, **4**, 2695.
- 42 H. Li, Q. Zhang, C.C.R. Yap, B.K. Tay, T.H.T. Edwin, A. Olivier, et al. *Adv. Funct. Mater.*, 2012, **22**, 1385.

Graphical abstract